The University Of Sheffield.

This is a repository copy of *Progress on Combined Load-and Profile-Control for Horizontal-Turret, Single-and Double-arm Tunnelling Machines*.

White Rose Research Online URL for this paper:
http://eprints.whiterose.ac.uk/76902/

Monograph:
Edwards, J.B. and Sadreddini, S.M. (1985) Progress on Combined Load-and Profile-Control for Horizontal-Turret, Single-and Double-arm Tunnelling Machines. Research Report. Acse Report 276 . Dept of Automatic Control and System Engineering. University of Sheffield

---

Reuse
Unless indicated otherwise, fulltext items are protected by copyright with all rights reserved. The copyright exception in section 29 of the Copyright, Designs and Patents Act 1988 allows the making of a single copy solely for the purpose of non-commercial research or private study within the limits of fair dealing. The publisher or other rights-holder may allow further reproduction and re-use of this version - refer to the White Rose Research Online record for this item. Where records identify the publisher as the copyright holder, users can verify any specific terms of use on the publisher's website.

Takedown
If you consider content in White Rose Research Online to be in breach of UK law, please notify us by emailing eprints@whiterose.ac.uk including the URL of the record and the reason for the withdrawal request.

White Rose university consortium
Universities of Leeds, Sheffield & York

eprints@whiterose.ac.uk
https://eprints.whiterose.ac.uk/

629.8(S)
[redacted]

PROGRESS ON COMBINED LOAD- AND PROFILE-CONTROL FOR HORIZONTAL-TURRET, SINGLE- AND DOUBLE-ARM TUNNELLING MACHINES

by

J. B. EDWARDS and S. M. SADREDDINI

Department of Control Engineering
University of Sheffield
Mappin Street, Sheffield S1 3JD

Research Report No. 276

April 1985

N.C.B. Research Contract No. PSD 19(84)

200038962

1. Introduction

This is the first progress report on investigations conducted by the authors entirely on NCB Research Contract No. PSD 19(84). The contract, which commenced 1 October 1984, follows on from Research Contract No. 226072, work on which was devoted to studies related specifically to the Cadley Hill machine and that on trial at Middleton Mine: both single-boom tunnelling machines of the horizontal-turret type (Fig.1a). The investigations were aimed primarily at achieving stable load-control whilst cutting the outer circular portion of the tunnel profile i.e. with the boom-elevation (or range) held constant whilst the turret is rotated. Following analysis, simulation[1,2] and redesign work[2,3,4], an existing load-control unit from the Middleton machine was modified at Sheffield and successfully tested on field trials[5] at Middleton. A specification for the redesign of the control units was then lodged with the suppliers, Dowty Electronics Ltd, for design modification and intrinsic-safety testing.

Because the Middleton machine is required to cut a flat floor, some preliminary investigation[4] of possibilities for making the load-controller cope with a cutting-trajectory of varying radius was undertaken leading to the conclusion that, as a minimum, some form of radius measurement must be used to modulate the parameters of the load-controller. The whole problem of interaction between load-control and profile-control was shown to require deeper investigation however. This conclusion was one factor leading to the present contract being placed. The development of other types of rock-cutting machine by MRDE and elsewhere and the widespread use of existing types of different design, notably vertical-turret machines (Fig.1b), (all ideally requiring load* control of some

---

*The term load is here used very generally to include all forms of load measurement including cutter-motor power or current, forces, torques or pressures in the boom- or head-drive mechanisms.

sort whilst cutting a variety of extraction profiles) was another factor. Of the new designs, the double-arm mechanism (Fig.1c) has been treated with some priority.

Because of the wide range of machine types (including horizontal-turret, vertical-turret and double-arm) it has been thought best to approach the problem in as general a manner as possible so that the final load-profile control system specification might cope with any machine type merely by the insertion of appropriate coordinate-conversion software. Since much experience had already been gained on horizontal-turret machines, this has been selected as the "basis machine" initially and coordinate-conversion applied to predict the behaviour of the double-arm mechanism. The horizontal turret's base coordinates are polar coordinates however (ie. radius, r and rotation angle, α) and it is thought that it might be preferable to change to the vertical-turret as the basis machine in future since this operates essentially in cartesian coordinates (ie. vertical height y and horizontal sweep x) which are perhaps more readily understood and useable for the entry (into the control-computer) of reference coordinates for the desired cutting-trajectory and finished tunnel-profile.

The present report describes in Section 2, the basic form of combined load-profile control system designed by the authors for horizontal-turret machines that might be readily adapted for other mechanisms. Simulation results are given for the system algorithm coupled to a much simplified model of the machine's cutting dynamics.

In Section 3 the double-arm mechanism is analysed and simulations presented showing the movement of the two arms and the torques developed at the pivots. In Section 4 proposals for the direction of future work are presented. References to previous work are given in Section 5.

2. Combined Load- and Profile-Control (Horizontal-Turret Machines)

Once the boom is driven in two separate directions simultaneously, the load-control problem takes on a far greater complexity then when only a single boom drive is operating. If the boom were required to travel only in radial directions or along circular arcs centred on the turret's axis of rotation, then it is easy to envisage a load-control system (like that designed for Middleton) being switched between the elevation- and rotation-servos as appropriate, (perhaps with some change of controller-parameter-settings on changeover). When following other trajectories e.g. to form a horizontal floor or a straight tunnel-side, then both servos must be modulated by the measured load signal since both drives affect the cutter-motor power consumption. In addition however, both servos must be driven by the profile-control system in an attempt to achieve the desired, pre-stored, trajectory. The problem is how to combine the profiler and load control demands on each servo such that the control requirements of both are satisfactorily achieved.

Two schemes have been investigated, the first (scheme 1) in Research Report 242 and scheme 2 during the present project. Scheme 1 is therefore outlined only briefly here. It is inferior to scheme 2.

2.1 Scheme 1

The idea underlying this scheme is that the measured power signal should be split into two components P_1 and P_2 where P_1 is the component resulting from the rotational velocity $v_1 = r d\alpha/dt$ of the boom and P_2 from the radial velocity $v_2 = dr/dt$. Component P_1 is then used to modulate the rotation servo and P_2 the elevation (ranging) servo. For the special case of cutting vertical sides or horizontal floors, the direction of net velocity v ($= \sqrt{v_1^2+v_2^2}$) can be readily related to measured rotation angle α (θ in RR 242) so allowing ready calculation of

P_1 and P_2 from the total power and angle measurements e.g. for a vertical downward trajectory

$$P_1 = P_m \cos^2 \alpha \qquad (1)$$

$$P_2 = P_m \sin^2 \alpha \qquad (2)$$

, where P_m = mechanical power delivered by cutting head motor. For general arbitrary profiles however, resolution of components P_1 and P_2 would need the direction of v to be determined from the two drive speed measurements or swash positions. The scheme as presented in RR 242 is therefore restricted to specific trajectories and is not easily generalised. In simulation, the two components of power error were weighted and combined additively with the relevant weighted profiler errors before application to the respective servo inputs. Although some success was achieved, it was found difficult to tune the system to give good load control and good profile control simultaneously over a range of conditions. Scheme 2 appears to be more generally applicable, easier to tune and more rationally based. It is described in the next Section 2.2.

2.2 Scheme 2

This scheme is shown in Fig.2 in block-diagram form and is flow-charted in Fig.3. The desired profile is defined by preloaded tables of α_r and r_r (= reference angles and radii respectively) stored to a base of ℓ_d = the desired distance to be travelled along the desired profile. Errors between desired and measured actual coordinates are presently used to proportionally control the two servos thus

$$u_\alpha = k_{p\alpha} (\alpha_r - \alpha) \qquad (3)$$

$$u_r = k_{pr} (r_r - r) \qquad (4)$$

where u_α and u_r are the inputs to the elevation- and rotation-servos respectively and $k_{p\alpha}$ and k_{pr} are the proportional profiler gains. More elaborate control laws could be used. All that is needed to drive this profiler system is input ℓ_d (to step the reference tables) and this is readily obtained by integration of desired cutting head speed v_d within the computer:

$$\ell_d = \int_o^t v_d dt \qquad (5)$$

The signal v_d can be either manually set or, for auto load-control, calculated from the measured power error by an appropriate control law. Present simulation studies have been limited to very simple cutting dynamics

$$P_i = P_m = k_h/(1+T_c s) \qquad (6)$$

where k_h is a hardness factor and T_c related to the interval between cutting picks and, for this, a proportional control law suffices, viz:

$$v_d = k_\ell (P_r - P_i) \qquad (7)$$

When full cutting dynamics and boom structural dynamics[5] are included then the more elaborate load-control algorithm designed for the Middleton and Cadley machines would be needed but should suffice.

2.3 Results

Figs. 4 to 7 inclusive show typical responses obtained from simulation of the load/profile control system of scheme 2 coupled to the simple cutting dynamics of equation 5 and hydraulic servo models described by identical first-order lags:

$$D\alpha = u_\alpha/(1+T_h D) \qquad (8)$$

$$Dr = u_r/(1+T_h D) \qquad (9)$$

The process parameters used were T_c = 1.67s, k_h = 6460 kW/m/s, P_r = 250kW, hydraulic time-constants T_h = 0.1s whilst the control parameters $k_{p\alpha}$, k_{pr} and k_ℓ were as indicated in the responses. The D-shaped cutting-trajectory α_r and r_r was prestored from analytic formulae in two 600 increment arrays with distance-sampling every 3cm and the simulation time-step was 0.05s. A step increase in hardness factor k_h of 50% is applied shortly before the top of the arch (traversed counterclockwise) in Fig.4 and the resulting speed reduction is clearly shown whilst the power is only slightly increased after a short transient following the disturbance. Other similar transients in the load trace are noticeable at points where the trajectory passes through discontinuities (corners).

As would be expected, the profile-following accuracy increases with increasing $k_{p\alpha}$ and k_{pr} but at the expense of somewhat increased disturbance on the load trace at the corners and increased ripple due to the discrete sampling of the reference profile. This is not thought to be too serious however, since some prior filtering of the stored reference tables and increased resolution (e.g. 10 times) would reduce the effect without difficulty and without excessive storage problems (12 kbytes).

Of some concern is the large velocity surge (Figs. 4 and 5) at start-up in some cases when the boom starts very close to the machine centre. This is thought to be due to the asymmetry of the overall system (Fig.2) which would not be present in an x,y (vertical turret) system. Further investigation is proceeding. Overall the results demonstrate the fundamental soundness of the scheme and this has been further confirmed in following alternative cutting trajectories.

3. Modelling the Double Arm Mechanism

3.1 Arm positions

As a first step in simulating the double arm mechanism the necessary coordinate conversion formulae between (θ,ϕ) (Fig.1c) and (r,α) were determined from the trigonometry of Fig.8. Given θ and ϕ, r and α may be evaluated from the following algorithm {(10) to (20)}, knowing the lengths ℓ_1 and ℓ_2 of the primary and secondary arms:

$$Z = \ell_2 \sin \phi \tag{10}$$

$$W = \ell_2 \cos \phi \tag{11}$$

$$\gamma' = \tan^{-1}|z/(w+\ell_1)| \tag{12}$$

$$\gamma = \gamma', \; z \geq 0, \; w+\ell_1 > 0 \tag{13}$$

$$\gamma = \pi-\gamma', \; z \geq 0, \; w+\ell_1 < 0 \tag{14}$$

$$\gamma = 2\pi-\gamma', \; z < 0, \; w+\ell_1 > 0 \tag{15}$$

$$\gamma = \pi+\gamma', \; z < 0, \; w+\ell_1 < 0 \tag{16}$$

$$\gamma = \pi/2, \; z > 0, \; w+\ell_1 = 0 \tag{17}$$

$$\gamma = 3\pi/2, \; z < 0, \; w+\ell_1 = 0 \tag{18}$$

$$r = \sqrt{\ell_1^2+\ell_2^2+2\ell_1\ell_2\cos \phi} \tag{19}$$

$$\alpha = \theta+\gamma \tag{20}$$

The solutions for r and α given by equations (10) to (20) are, of course, unique. Reverse conversion, from given coordinates r and α, to obtain θ and ϕ requires the following algorithm {(21) to (31)}:

$$C_\gamma (= \cos \gamma) = (r^2+\ell_1^2-\ell_2^2)/2r\ell_1 \tag{21}$$

$$S_\gamma (= \sin \gamma) = + \sqrt{1 - C_\gamma^2} \tag{22}$$

$$\gamma = \tan^{-1}|S_\gamma/C_\gamma| \quad , \quad C_\gamma > 0 \tag{23}$$

$$\gamma = \pi-\tan^{-1}|S_\gamma/C_\gamma| \quad , \quad C_\gamma < 0 \tag{24}$$

$$\gamma = \pi/2 \quad , \quad C_\gamma = 0 \tag{25}$$

$$z = r\,S_{\gamma} \tag{26}$$

$$w = rC_{\gamma} - \ell_1 \tag{27}$$

$$\theta = \alpha - \gamma \tag{28}$$

$$\phi = \tan^{-1}|z/w| \quad , \quad w > 0 \tag{29}$$

$$\phi = \pi - \tan^{-1}|z/w| \quad , \quad w < 0 \tag{30}$$

$$\phi = \pi/2 \quad , \quad w = 0 \tag{31}$$

For given (r,α) there are of course two possible solutions for (θ,ϕ) in practice depending on whether the pivot P lies to the left or right of radius arm CD (Fig.8). The algorithm above assumes right-handed orientation.

The double arm simulation developed so far applies the two coordinate conversion routines (above) as indicated in Fig.9 to adapt the basic machine (horizontal turret) to the double arm. Algorithm (10) to (20) is used for inputing manual demands θ_r and ϕ_r from potentiometers (simulating the manual controls on the main and secondary (pivot) drives M_1 and M_2 shown in Fig.1c) into prestored reference tables r_r and α_r to allow a driver practice in constructing a desired cutting trajectory manually from these controls. Algorithm (21) to (31) is used, also as shown in Fig.9, to convert the polar coordinates r and α produced by the simulation previously described in Section 2, into coordinates θ and ϕ for display of pivot point P (Fig.1c and Fig.8). The graphics output links centre C to pivot P, and pivot P to drum centre D by straight lines to show the changing position of the two arms, (a) in setting up the desired trajectory and (b) in following this during the cutting simulation under the control described in Section 2.

Other forms of control e.g. using the torque τ_2 measured at the pivot to adjust the M_2 servo, as proposed by MRDE, have yet to be simulated. As a first step towards this, the formulae for calculation of the torques to be provided by motors M_1 and M_2 have been developed and programmed.

3.2 Torque Simulation

Fig.10a shows the two velocity components v_1 and v_2 due to rotation $d\alpha/dt$ and elevation dr/dt i.e.:

$$v_1 = r d\alpha/dt \tag{32}$$

$$v_2 = dr/dt \tag{33}$$

both produced in the simulation described in Section 2. The two components yield the net velocity v of the centre of the cutting-head, where

$$v = \sqrt{v_1^2+v_2^2} \quad , \quad \angle \psi = \psi_1+\alpha \tag{34}$$

where, if $\psi_1' = \tan^{-1}|v_1/v_2|$ (35)

then

$$\psi_1 = \psi_1' \quad , \quad v_1 \geq 0 \quad , \quad v_2 > 0 \tag{36}$$

$$\psi_1 = \pi-\psi_1' \quad , \quad v_1 \geq 0 \quad , \quad v_2 < 0 \tag{37}$$

$$\psi_1 = 2\pi-\psi_1' \quad , \quad v_1 < 0 \quad , \quad v_2 > 0 \tag{38}$$

$$\psi_1 = \pi+\psi_1' \quad , \quad v_1 < 0 \quad , \quad v_2 < 0 \tag{39}$$

$$\psi_1 = \pi/2 \quad , \quad v_1 \geq 0 \quad , \quad v_2 = 0 \tag{40}$$

$$\psi_1 = 3\pi/2 \quad , \quad v_1 < 0 \quad , \quad v_2 = 0 \tag{41}$$

Fig.10a also shows the two components of cutting force produced by v and drum rotation, namely F_1 opposing v and F_2 orthogonal to v, where

$$F_1 = k_{h1}\, v\, g_c(s) \angle \pi+\psi \tag{42}$$

and

$$F_2 = k_{h2}\, v\, g_c(s) \angle 3\pi/2+\psi \tag{43}$$

where $g_c(s)$ denotes the cutting dynamics ($= 1/(1+T_c s)$ in these preliminary studies but could be made more elaborate as in previous reports) and k_{h1} and k_{h2} are rock hardness coefficients related to k_h used previously. Parameter k_{h2} is positive if the drum rotation is counterclockwise but reverses sign on reversing drum rotation.

The resultant force F, as shown in Fig.10a is thus given by

$$F = \sqrt{F_1^2+F_2^2} \angle \pi+\psi+B \tag{44}$$

where, if angle B' is given by

$$B' = \tan^{-1}|F_2/F_1| \tag{45}$$

then
$$B = B' \quad , \quad F_2 \geq 0 \quad , \quad F_1 > 0 \tag{46}$$

$$B = \pi-B' \quad , \quad F_2 \geq 0 \quad , \quad F_1 < 0 \tag{47}$$

$$B = 2\pi-B' \quad , \quad F_2 < 0 \quad , \quad F_1 > 0 \tag{48}$$

$$B = \pi+B' \quad , \quad F_2 < 0 \quad , \quad F_1 < 0 \tag{49}$$

$$B = \pi/2 \quad , \quad F_2 > 0 \quad , \quad F_1 = 0 \tag{50}$$

$$B = 3\pi/2 \quad , \quad F_2 < 0 \quad , \quad F_1 = 0 \tag{51}$$

To find the torques τ_1 acting on centre shaft C and τ_2 acting on pivot P it is now merely necessary to resolve net cutting force F parallel and perpendicular to primary arm ℓ_1 yielding respectively components F_a and F_b (see Fig.10b) and then apply lever arms z and w already obtained from equations (26) and (27). More precisely:

$$F_a = F \cos(\pi-\psi-B+\theta) \angle \theta \tag{52}$$

$$F_b = F \sin(\pi-\psi-B+\theta) \angle \theta-\pi/2 \tag{53}$$

so that

$$\tau_1 = F_a Z + F_b(W+\ell_1) \tag{54}$$

$$\tau_2 = F_a Z + F_b W \tag{55}$$

3.2.1 Results of Torque Simulation

Fig.11 shows the torque traces produced with a counterclockwise rotating drum and a counterclockwise D-shaped reference trajectory of radius = 3m and vertical leg-length = centre-height = 2m. Power and

resultant velocity traces are also shown with the blips again indicating the arrival of the cutting head at the corners. The parameters used were:

$$\ell_1 = 1.75\text{m} \quad , \quad \ell_2 = 2.6\text{m}$$

(i.e. both double the arm-lengths for the prototype machine to allow the excavation of the large 5m tunnel)

$$k_{h1} = 15{,}900 \text{ kN/m/s} \quad , \quad k_{h2} = 15{,}900 \text{ kN/m/s}$$

these figures being derived from a value of hardness-factor, $k_h = 5000$ kW/m/s from the formulae:

$$k_{h1} = k_h \frac{N\,T}{2\pi}\, r_h \qquad (56)$$

and $$k_{h2} = r_f\, k_1 \qquad (57)$$

where N = no of pick spirals/revolution = 6

T = time between successive spirals = 1.67s

r_h = cutting head radius = 0.5m

r_f = ratio between integrated circumferential/radial cutting-force components = 1.0

Controller parameters were:

$$k_\ell = 1.5\ 10^{-3} \text{ m/s/kW}$$

$$k_{p\alpha} = 0.2\ s^{-1} \quad , \quad k_{pr} = 0.2\ s^{-1}$$

Critical values of τ_1 can be readily checked for accuracy, e.g. during the arc-cutting (0° to 180°) $\tau_1 = k_{h1} v x 3 = 15{,}900 x 0.034 x 3 = 1619$ kNm as shown. During the interval 180° to 225° the net force on the drum $= \sqrt{2}\, k_{h1} v$ and is at an angle of 135° and the lever-arm would become $\sqrt{2}$x3m if the leg-length were 3m giving a torque $\tau_1 = 2x1619 = 3238$ kNm on reaching the bottom of such a leg. In our case the leg-length = only

2m so that the torque does not build up to quite this value. The collapse of the torque after the bottom L.H. corner is caused by the lever-arm falling to a slight negative value as the net force direction changes to 225^{o}, the lever-arm then increasing linearly to its previous value by the time the bottom R.H. corner is reached. τ_1 thus reaches the same value at this corner as at the bottom L.H. corner. The fall of τ_1 to a low positive value at the start of the vertical climb is explained by the fact that the net force of $\sqrt{2}\ k_{h1} v$ is now inclined at 315^{o} so that the lever-arm is only a small positive value immediately after the corner. Thereafter τ_1 increases towards its original value as expected as the lever arm increases.

Similar arguments can be used to validate the τ_1-response shown in Fig.12 for identical parameters but with a clockwise-rotating head (i.e. $k_{h2} = -15{,}900$ kN/m/s).

The τ_2-traces are validated with more difficulty but, due to close relation between equations (54) and (55), it would seem unlikely that programming errors could have occurred making τ_1 correct whilst τ_2 is incorrect.

4. Discussion and Future Work

The basis of a scheme for simultaneous load and profile control has been demonstrated. The scheme utilises reference tables of the two spatial coordinates (x_r, y_r for a vertical turret machine, α_r, r_r for a horizontal turret and θ_r, ϕ_r for a double arm mechanism) are tabulated to a basis of ℓ_d = the desired distance to be travelled along the desired trajectory. ℓ_d is found from integrating either the manual cutting speed demand or the demand produced by the load-control algorithm which would differ little from that originally designed and tested for the Middleton machine. Attention should now be focussed on how best to load

the reference tables into the computer arrays i.e. from analytic formulae, from driver teaching or some combination of both.

The tendency of the horizontal turret machine to fly at low initial radius needs some attention and is probably tied up with the lack of symmetry of the control system between the r- and α-loops (an assymmetry not present in x,y machines and which may also be a problem in θ, ϕ machines). There is probably some connection also with the possibility of huge forces developing in the horizontal turret mechanism at low radius.

Having established a completely symmetrical system for all machines, the individual servo dynamics should be modelled and simulated in detail and the full cutting dynamics included thereafter for a comprehensive test of the final universal specification. Towards including load and torque feedback for the double-arm mechanism, the simulation presented here has included computation of the torques on both main and secondary pivots. Their incorporation in feedback systems is to be investigated. It is interesting to note that under some circumstances, torques and rotational speeds may act in the same direction causing motors to pump fluid, though not simultaneously of course. A number of differences of opinion between ourselves and NCB with respect to force and torque directions require discussion in the near future.

5. References

These are all Research Reports of the Department of Control Engineering, University of Sheffield by J. B. Edwards and S. M. Sadreddini. The numbers, titles and dates are as follows:

(1) Research Report (R.R.) No.220, "Load control of a 300 h.p. tunnelling machine", April 1983.

(2) R.R. No.230, "Controller modification and testing for underground trials", June 1983.

(3) R.R. No.237, "The addition of integral control action to prevent manually-created overloads", August 1983.

(4) R.R. 242, "Control of load and profile in the machine-cutting of D-shaped tunnels: An initial investigation", Oct. 1983.

(5) R.R. 265, "Vibration due to the resilience of a tunnelling machine boom structure and its effect on load control", Sept. 1984.

SHEFFIELD UNIV.
APPLIED SCIENCE
LIBRARY

Fig.1. Types of Tunnelling Machine

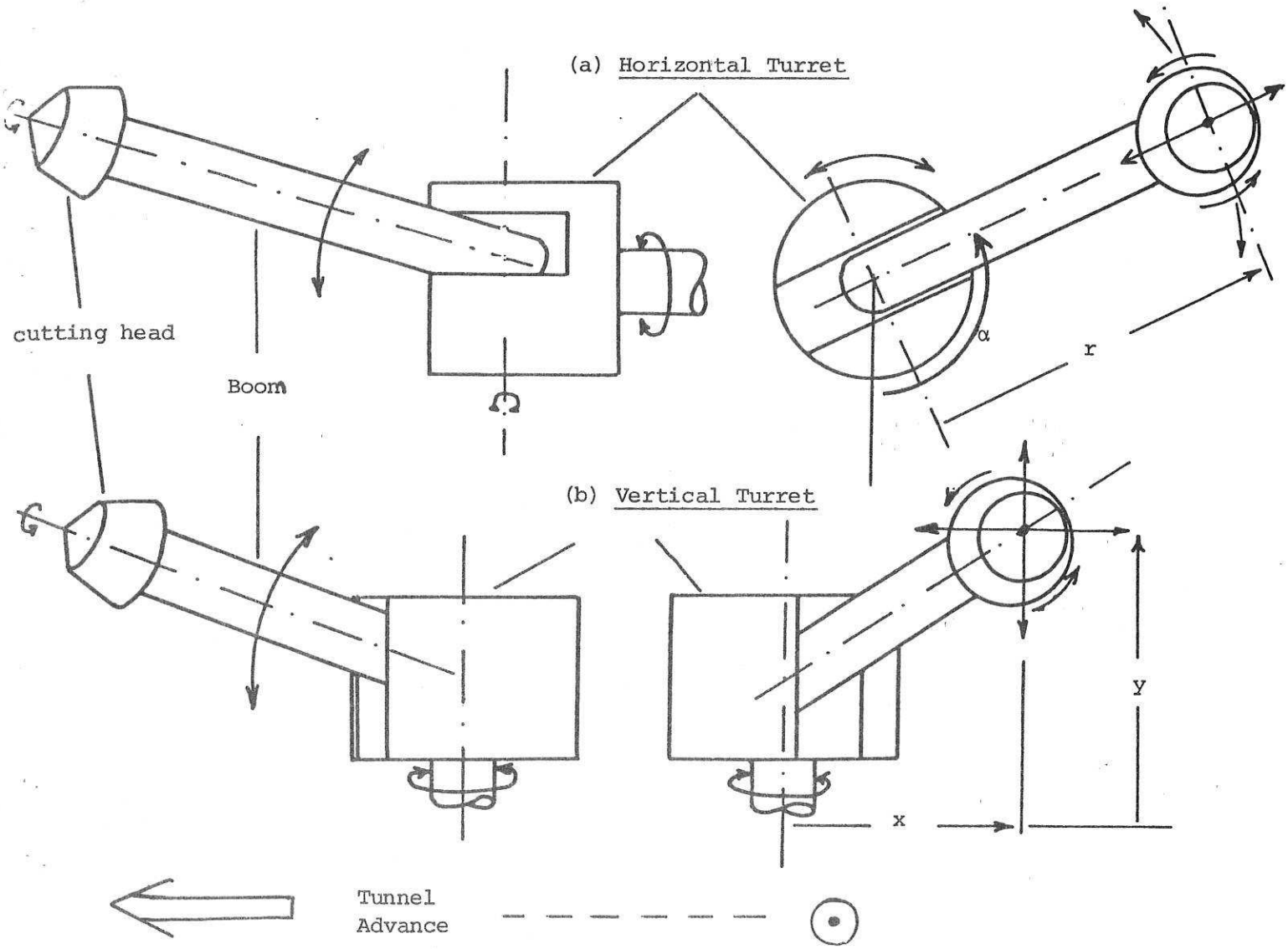

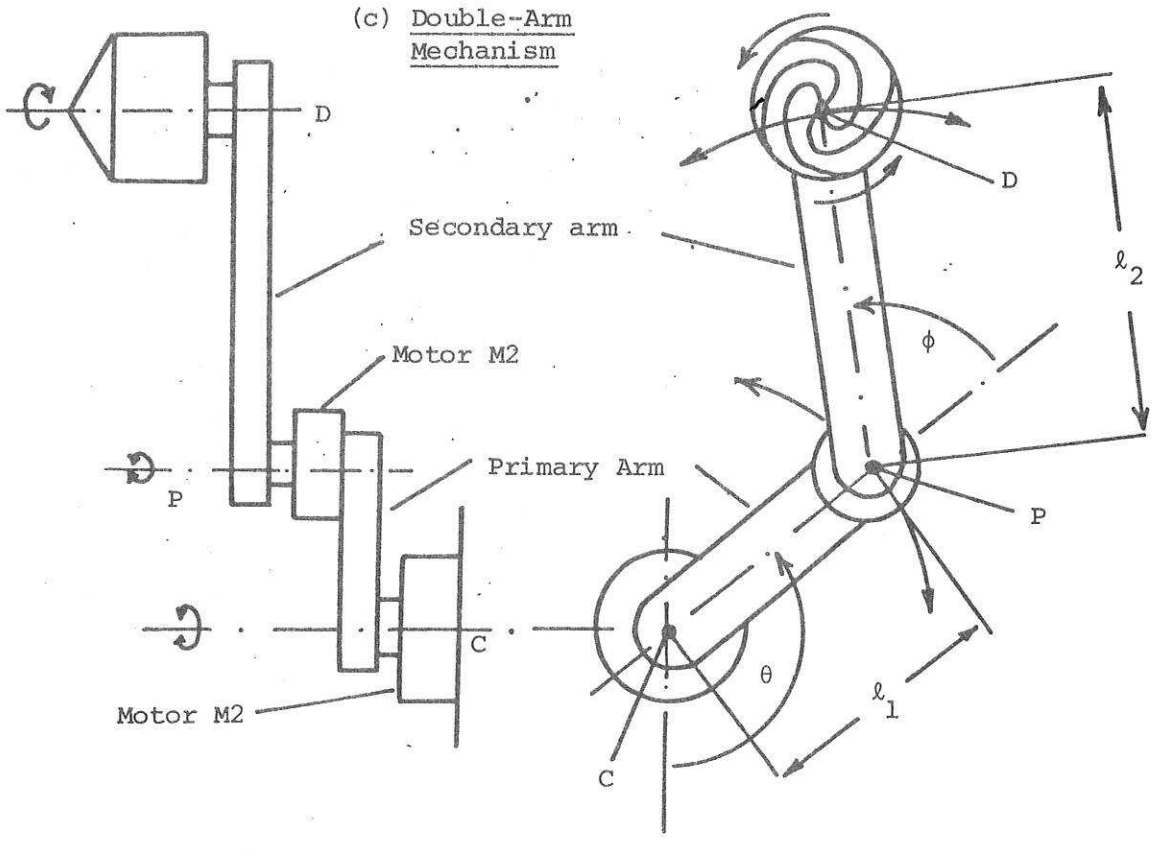

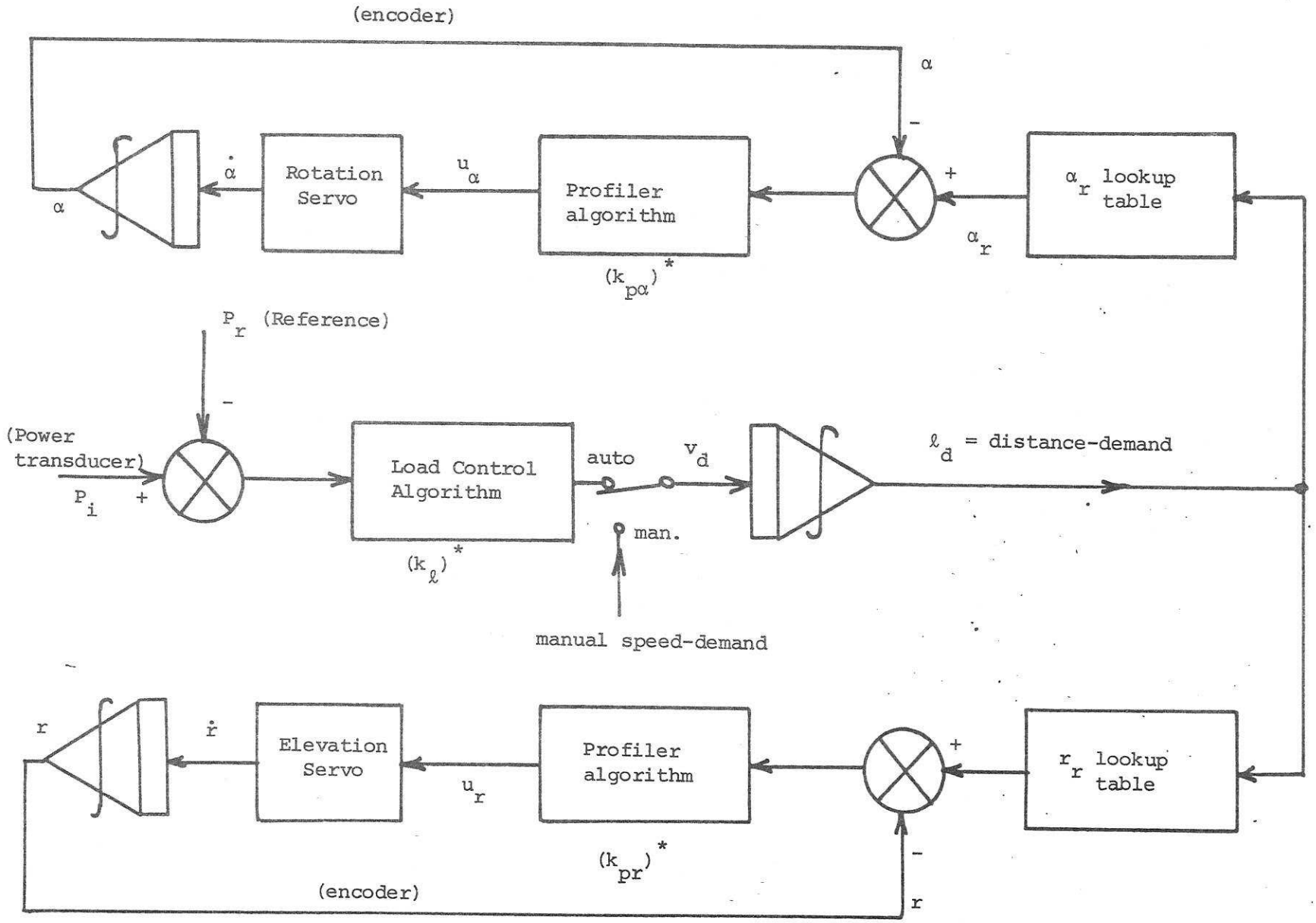

*Simple proportional control parameters used in preliminary simulations

Fig.2. Combined load/profile control scheme (2) (Schematic)

Fig.3. Combined load/profile control scheme: Flowchart

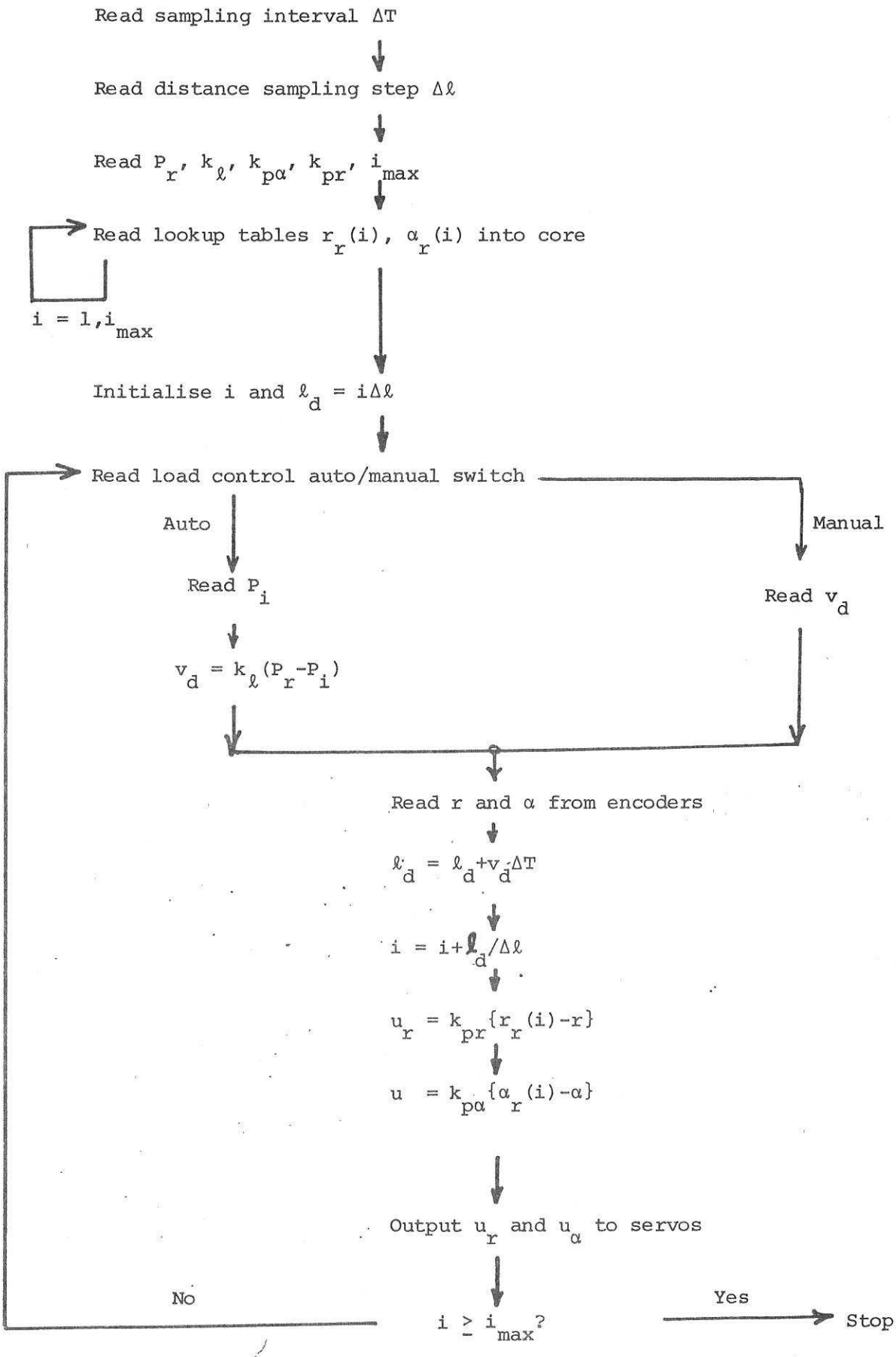

Simulation of Load & Profile Control

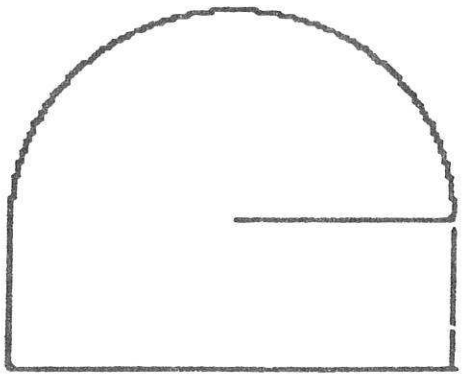

CTRL S for stop
CTRL Y for hardness
CTRL R for total samples

Do you wish to run the simulation again
(Y/N)■

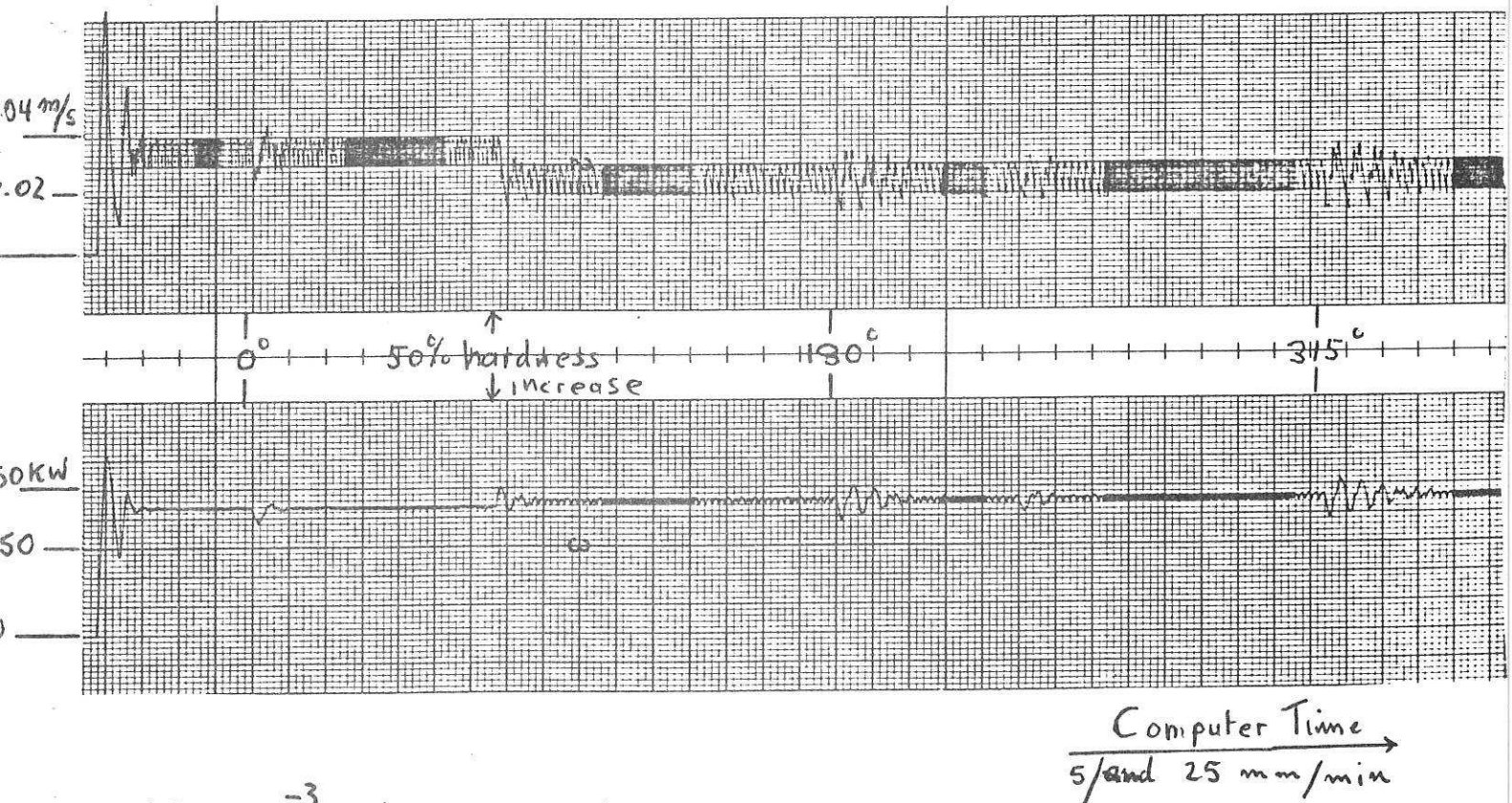

$k_f = 1.5 * 10^{-3}$ $k_{p\alpha} = 0.5$ $k_{pv} = 0.5$

Fig.4. Profile, speed and power responses for System 2

Simulation of Load & Profile Control

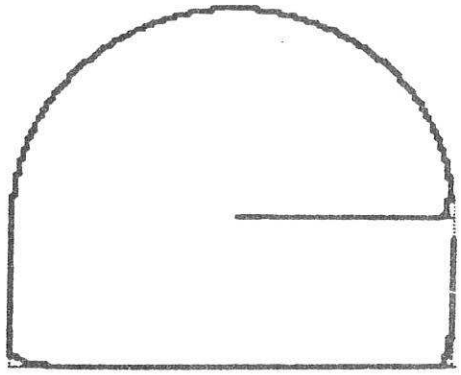

CTRL S for stop
CTRL Y for hardness
CTRL R for total samples

Do you wish to run the simulation again
(Y/N)■

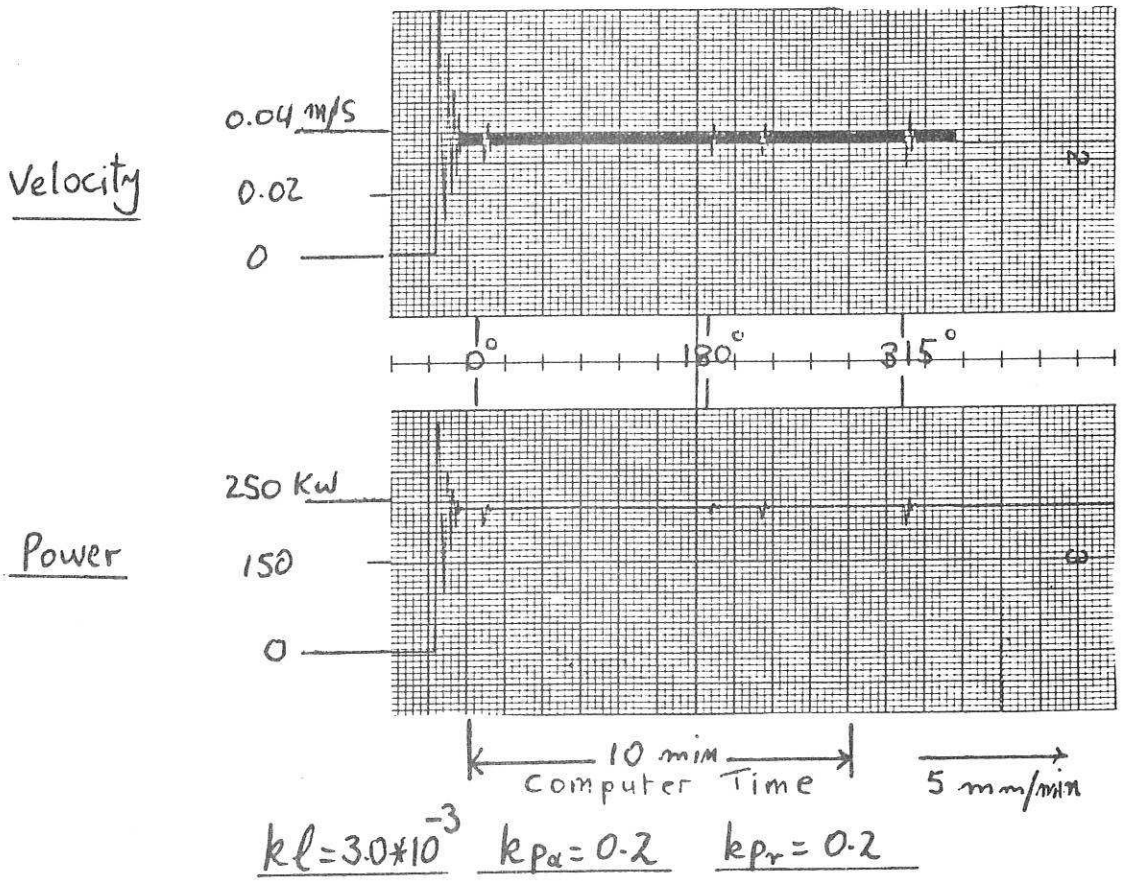

Fig.5. Profile, speed and power responses for System 2

Simulation of Load & Protile Control

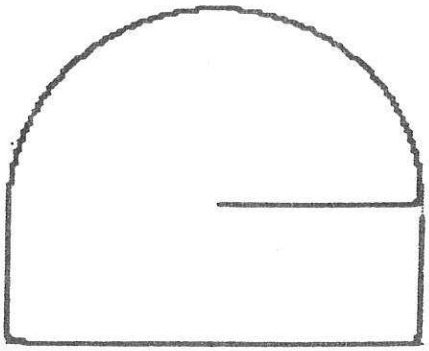

CTRL S for stop
CTRL Y for hardness
CTRL R for total samples

Do you wish to run the simulation again
(Y/N)■

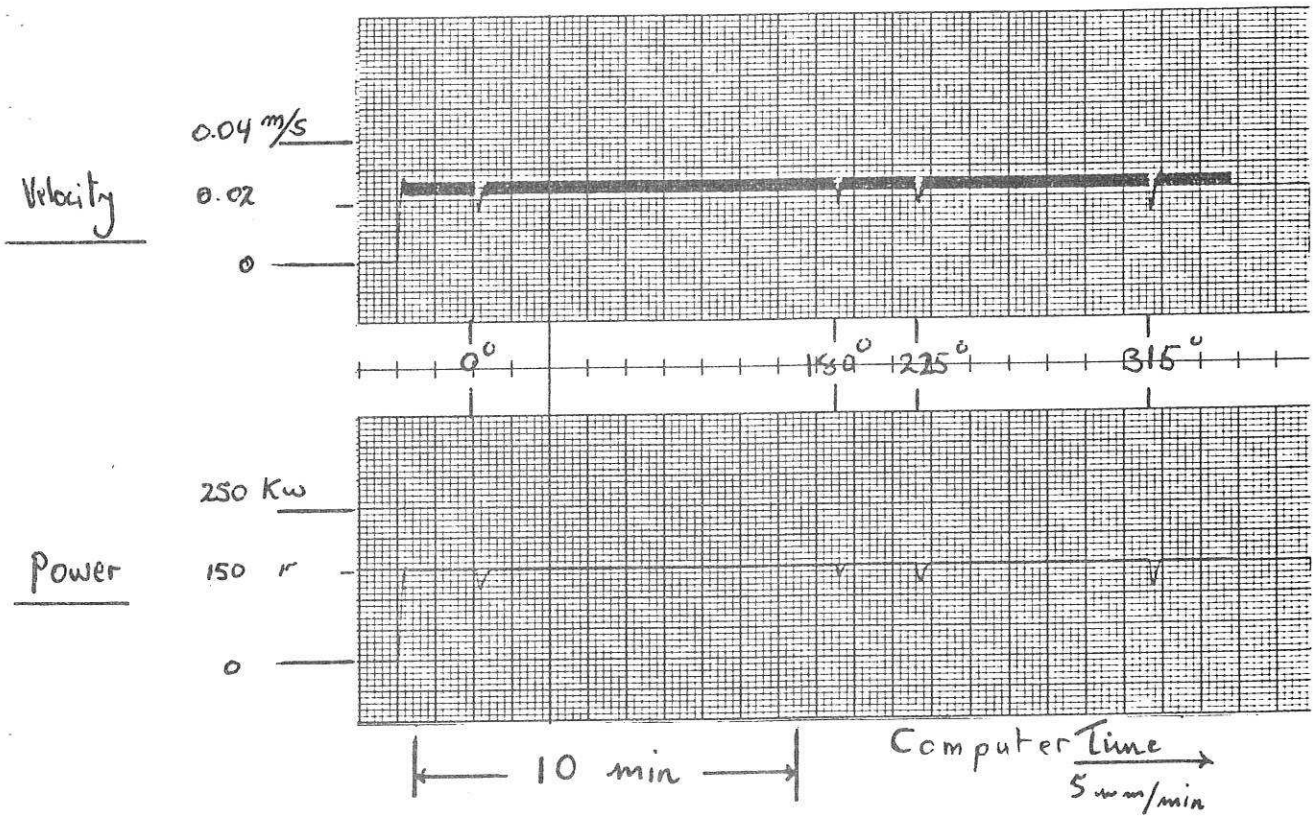

Fig.6. Profile, speed and power responses for System 2

Simulation of Load & Profile Control

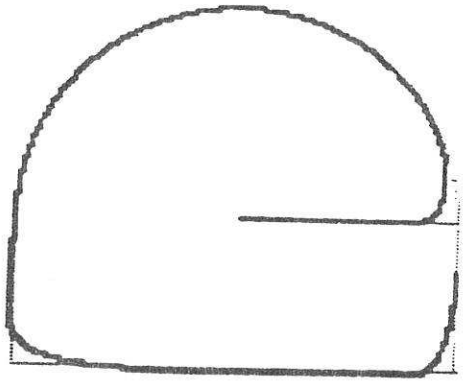

CTRL S for stop
CTRL Y for hardness
CTRL R for total samples

Do you wish to run the simulation again
(Y/N)■

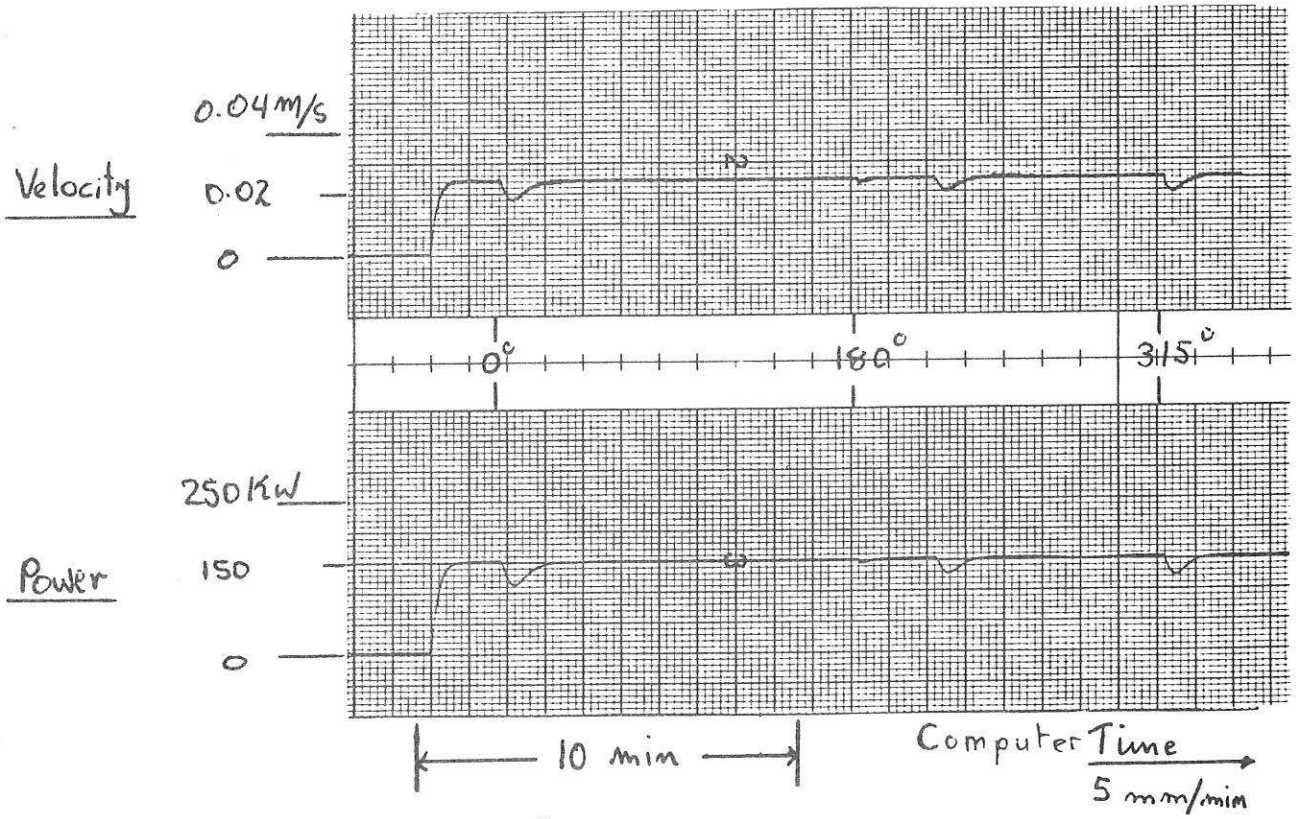

$k\ell = 3.0 \times 10^{-4}$ $k p_\alpha = 0.05$ $k p_n = 0.05$

Fig.7. Profile, speed and power responses for System 2

Fig.8. Geometry of Double-Arm Mechanism

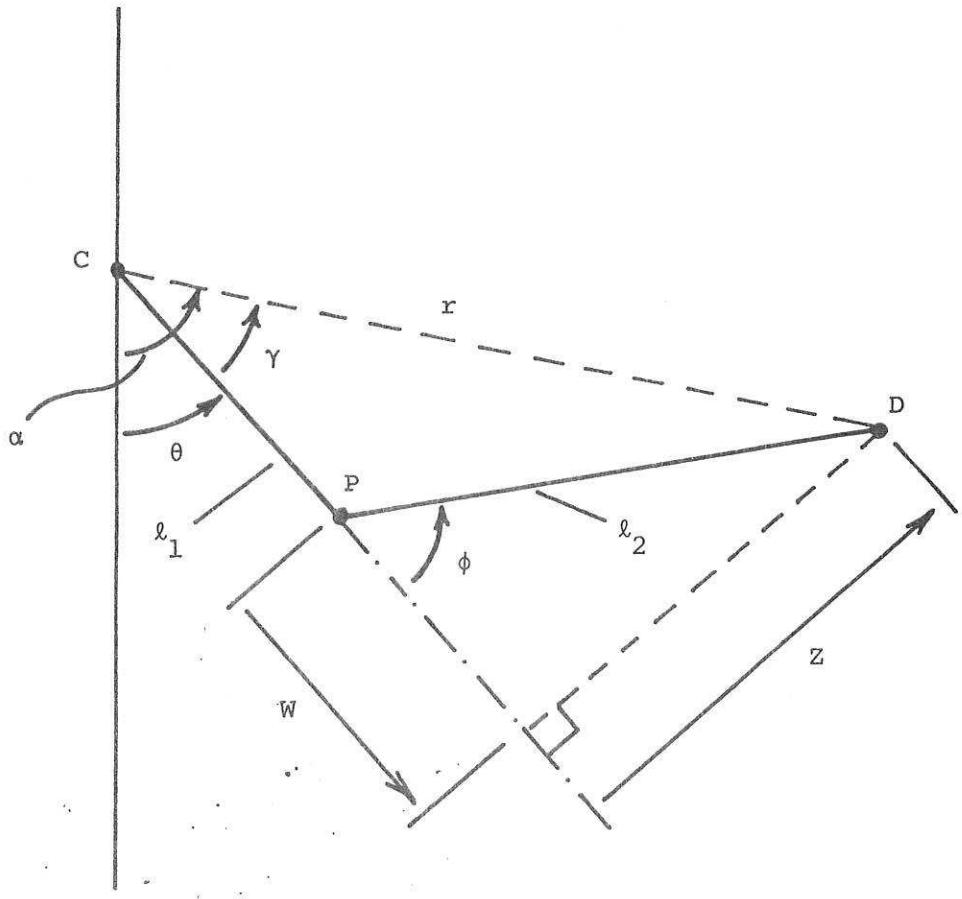

C = machine centre

P = pivot

D = drum

Fig.9. Showing use of $(r,\alpha)/(\theta,\phi)$ coordinate conversion routines in overall simulation scheme

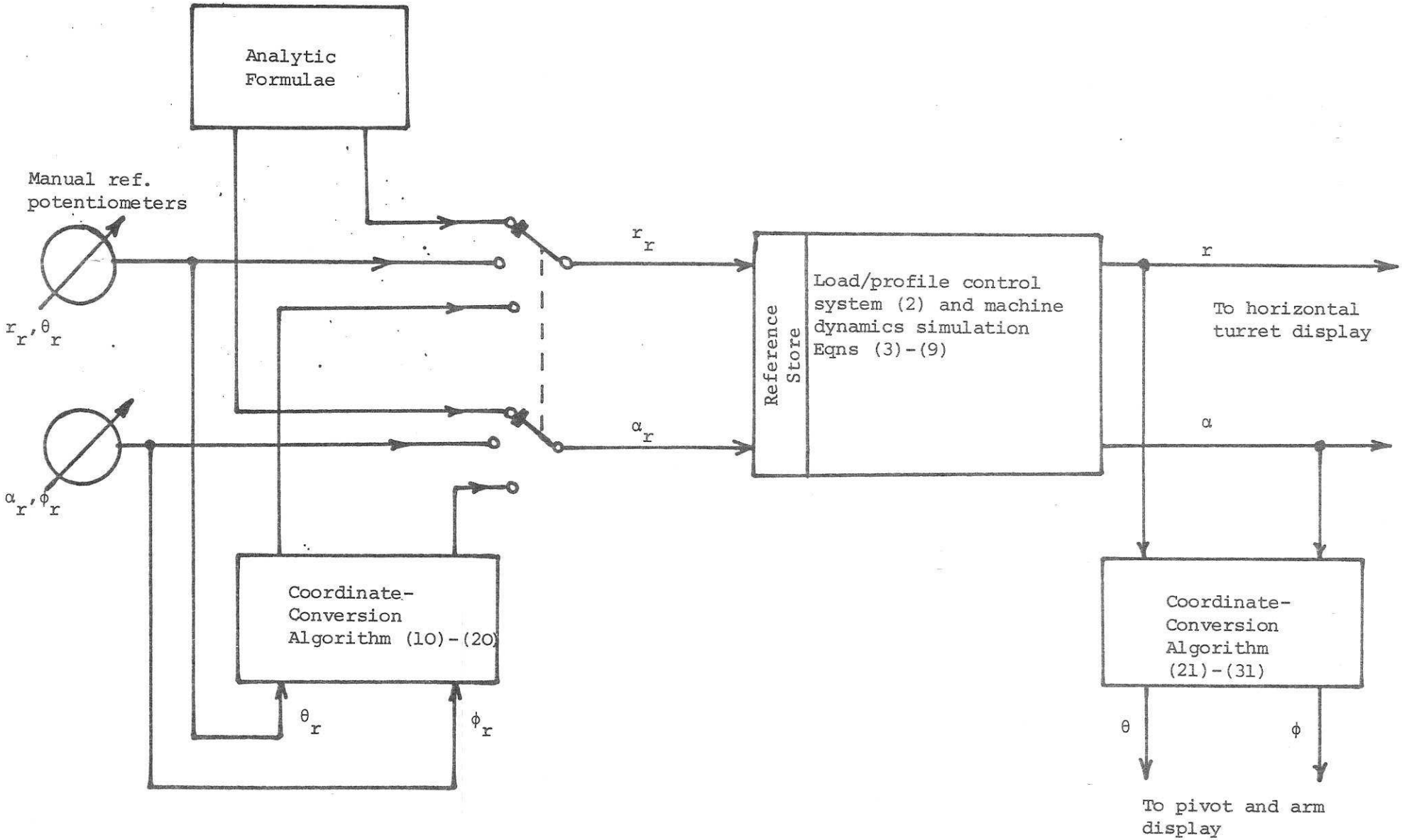

Fig.10a. Showing cutting-forces produced by radial and tangential velocities

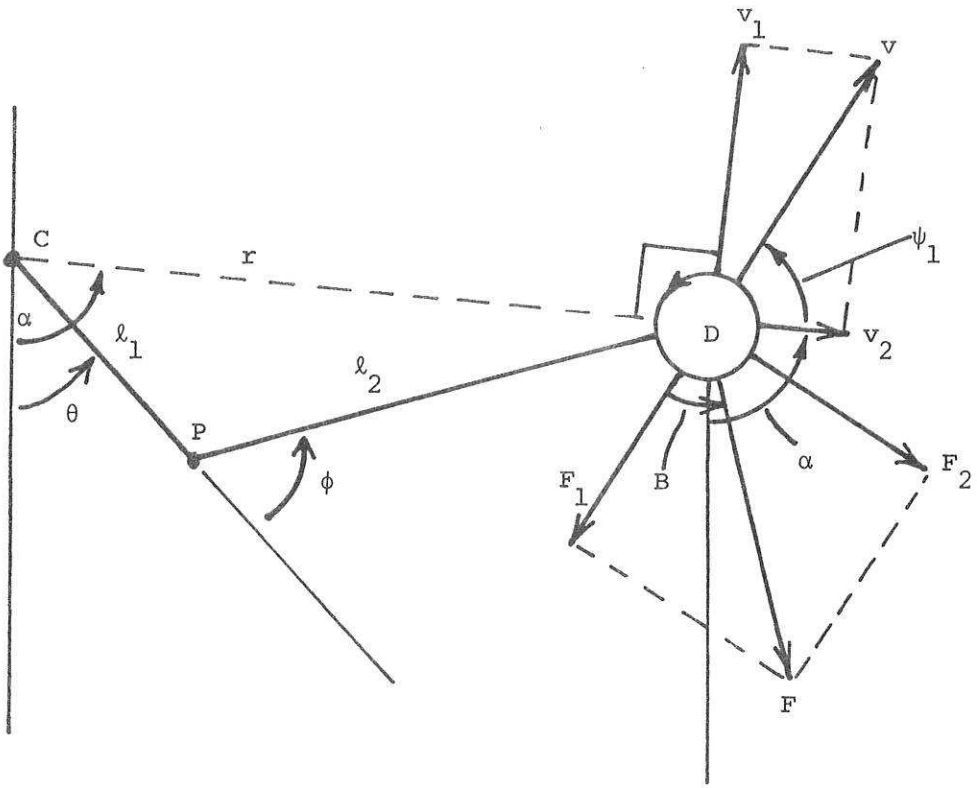

Fig.10b. Resolving net force parallel and perpendicular to primary arm

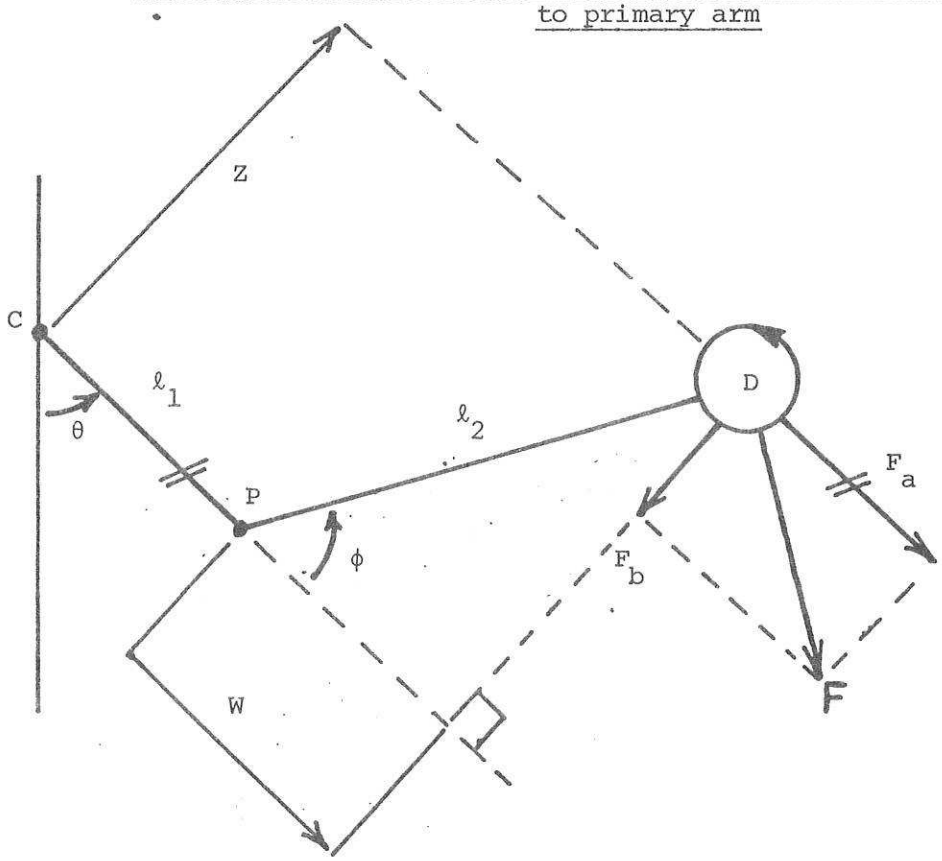

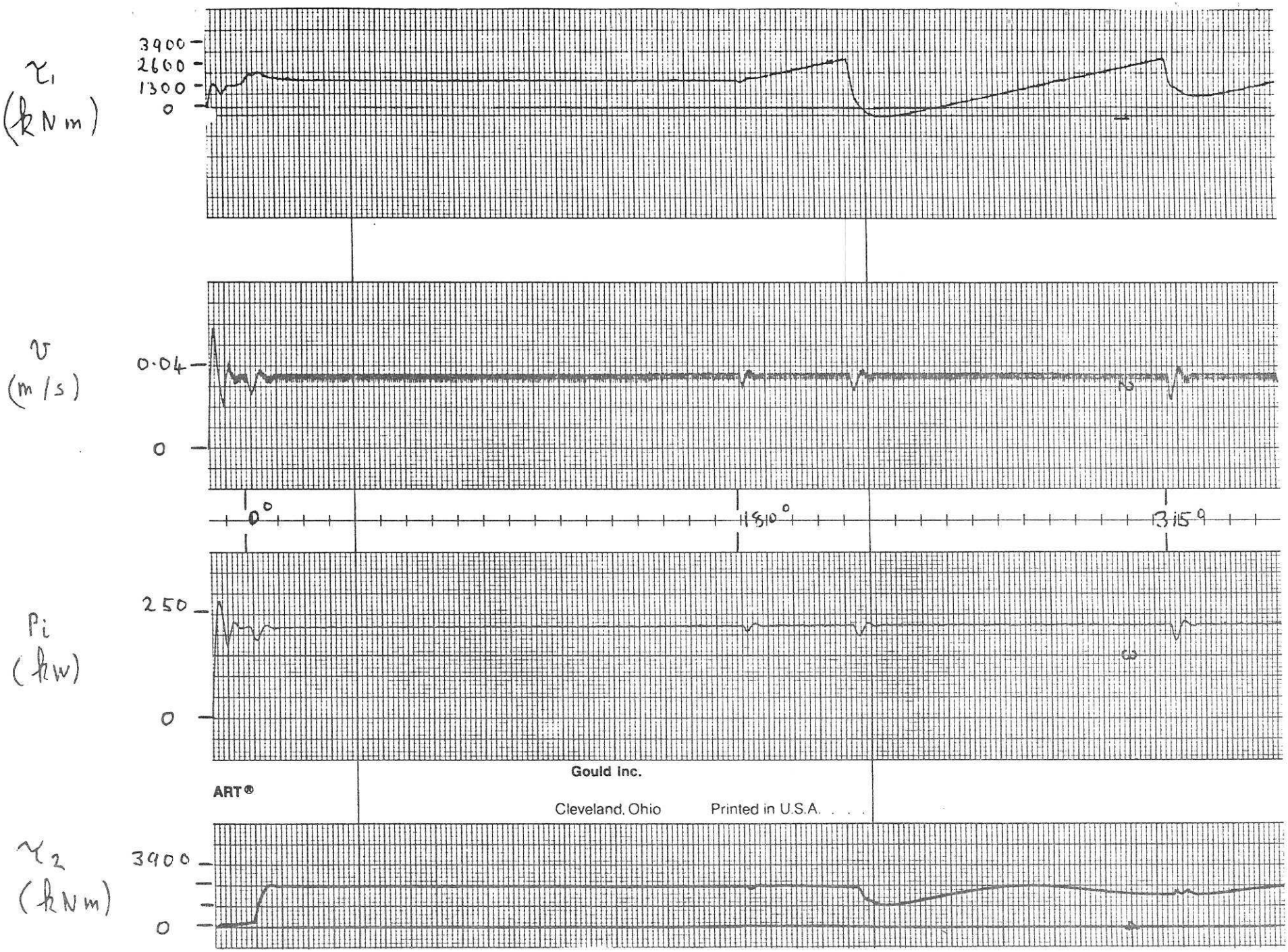

Fig.11. Torque, speed and power responses of double arm mechanism with counterclockwise drum rotation

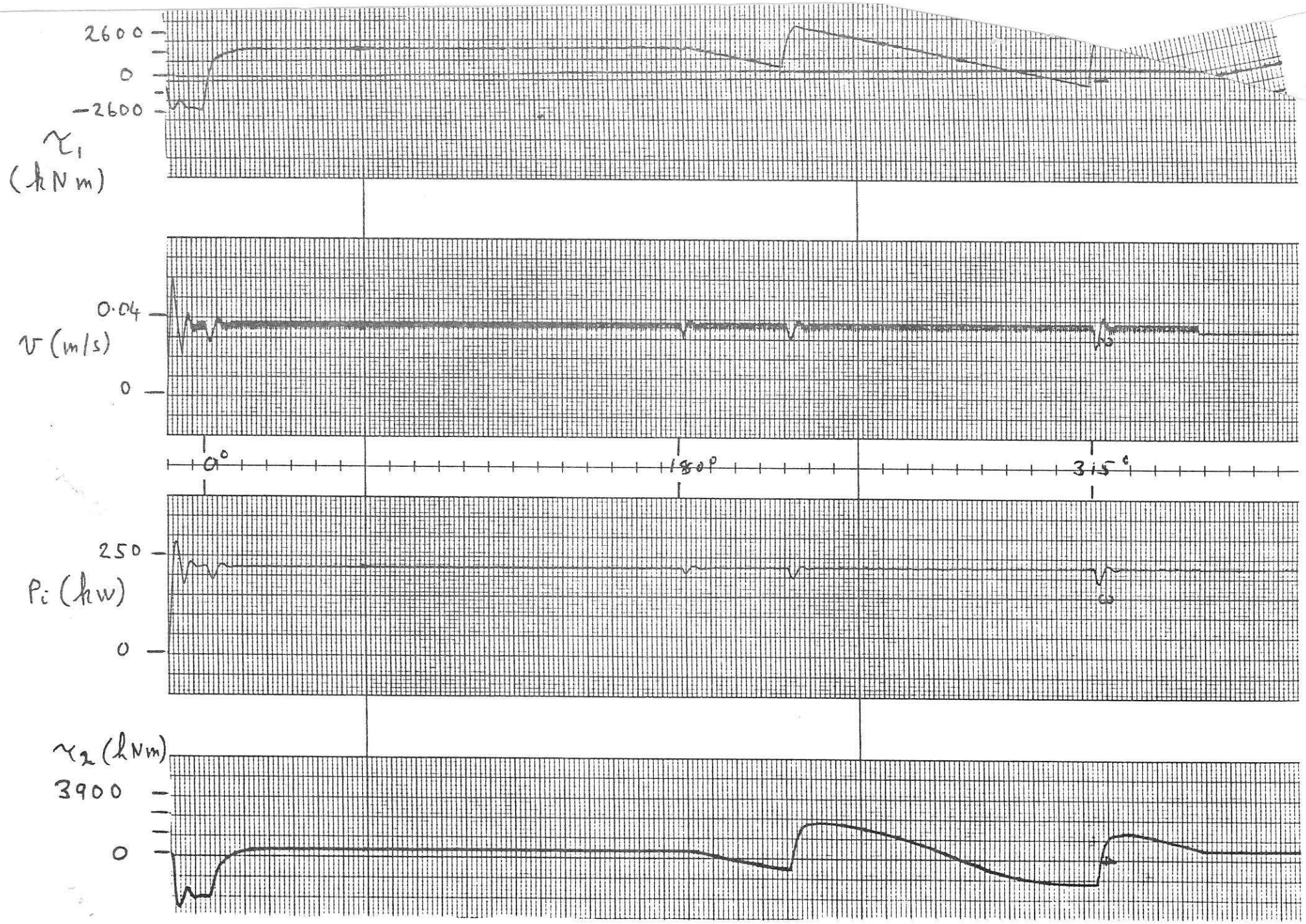

Fig.12. Torque, speed and power responses of double arm mechanism with clockwise drum rotation